Segmentation of Substantia Nigra using Weighted Thresholding Method

Dibash Basukala
Department of Computer Science and Software Engineering, University of Canterbury
Christchurch, New Zealand
dibash.basukala@pg.canterbury.ac.nz

Ramakrishnan Mukundan
Department of Computer Science and Software Engineering, University of Canterbury
Christchurch, New Zealand
mukundan@canterbury.ac.nz

Tracy Melzer
New Zealand Brain Research Institute, Department of Medicine, University of Otago
Christchurch, New Zealand
tracy.melzer@otago.ac.nz

Ross Keenan
New Zealand Brain Research Institute, Pacific Radiology
Christchurch, New Zealand
ross.keenan@pacificradiology.com

***Abstract*— Substantia nigra (SN) located in the midbrain can provide significant information about the Parkinson's disease (PD) characteristics and progression as it is highly correlated to PD. Therefore, accurate segmentation of SN is crucial in computer-aided diagnosis of PD. There exists a limited number of methods proposed for SN segmentation, as it can only be visualized by high quality imaging method and it is a fairly recent development. Most of the existing methods for SN segmentation requires number of expert supervised reference images for increasing accuracy and are also computationally expensive. Therefore, we propose a novel algorithm for the segmentation of SN using thresholding operation. Threshold value is estimated based on the *k*-means algorithm on different samples of the image including cross-diagonal pixels and the pixels outside the cross-diagonals. The final threshold value required for the accurate segmentation of SN is calculated as the weighted sum of threshold estimated along the cross-diagonal pixels and the pixels outside the cross-diagonals. The experimental results suggest that the proposed method is capable of segmenting SN closer to manual delineation. The subjective evaluation performed by the radiologist supports our claim. Moreover, the proposed methodology is also compared with general thresholding methods and level set method to show the superiority of our proposed algorithm.**

Keywords— Segmentation, Parkinson's disease, thresholding, k-means, substantia nigra.

I. Introduction

Parkinson's disease (PD) is a neurodegenerative disease characterized by many movement disorders including rigidity, tremor, akinesia, poor balance and motor coordination. It is correlated to the neuronal loss of dopamine (DA) in substantia nigra (SN) pars compacta [1].

Conventional magnetic resonance imaging (MRI) at standard field strength fail to visualize the structure of SN because of the insufficient contrast-to-noise ratio and spatial resolution. But, advanced MR imaging technique at 7 Tesla (T) have improved signal-to-noise ratio to increase the spatial resolution and therefore smaller brainstem nuclei like SN can be visualized. SN is an iron rich structure [2, 3] clearly visible in T2-weighted and T2*-weighted images.

Segmentation of SN can provide insight to PD characterization [4] and progression and can be used in numerous clinical and research applications including volumetric measurement, three-dimensional visualization, early disease diagnosis and detection of changes over time. However, segmentation of SN is a difficult task because of the smaller structure, unclear boundaries, morphometric variability and similar intensity with the adjacent structures. Automated segmentation method is capable of giving more consistent results to manual segmentation because of the absence of operator bias in addition to saving time and labor. There exists limited number of literature for the SN segmentation because high quality imaging capable of visualizing SN is a fairly recent development.

Xiao et al. [5] proposed the segmentation of smaller brainstem nuclei by incorporating multiple MRI contrasts which includes T1-weighted and T2*-weighted images into a single image for better non-rigid registration of atlas to achieve higher segmentation accuracy. Haegelen et al. [6] compared the manual segmentation with two registration based methods; automatic nonlinear image matching and anatomical labeling (ANIMAL) and symmetric image normalization (SyN) which are performed on T1-weighted images. Additionally, they also compared with patch based method applied on T2-weighted images. Xiao et al. [7] described the label-fusion segmentation using majority-voting approach for the segmentation of the midbrain nuclei and also measured morphometric variability by using principal component analysis (PCA). Kim et al. [8] combines an active surface model and prior shape knowledge for the semiautomatic segmentation of subcortical structures. Visser et al. [9] described an intensity model and a shape model based on Markov random field (MRF) for the automatic segmentation of smaller brain nuclei. Also, Guo et al. [10] combines atlas registration, seed points discontinuity and level set method for the segmentation of cerebral nuclei.

However, the morphometric variability of SN limits the accuracy of segmentation in atlas based methods which is one of the most popular method for SN segmentation. Similarly, majority of the method proposed in the literature requires number of expert supervised reference images to increase the labeling accuracy. However, the segmentation results are still not free from error. Additionally, it also

978-1-7281-0125-5/18/$31.00 ©2018 IEEE

increases the computational cost which is not always favourable.

Therefore, to address the problem and challenges of the existing segmentation algorithms, we propose and evaluate a new and improved algorithm for the segmentation of SN in T2*-weighted images based on the thresholding approach. The region of interest (ROI) is selected from the input brain MRI. *K*-means algorithm is applied on different samples of ROI image including cross-diagonal pixels and the pixels outside the cross-diagonals to compute the threshold value along each of these samples. The threshold estimated along the cross-diagonal pixels and the pixels outside the cross-diagonals are weighted to calculate the final threshold value for the accurate segmentation of SN which in turn will help clinicians in the diagnosis of PD. The flowchart of the proposed method is shown in Fig. 1. The details of the proposed methodology will be discussed in the next section.

II. Materials And Methods

A. K-means Algorithm

K-means [11-14] algorithm is a popular unsupervised method which is widely used because of its simplicity. It partition the ROI intensities into k clusters and aims to minimize the sum of squared distance between the data points and the cluster center. The main steps of the k-means algorithm to partition the ROI intensities y_i, $i=1,2,3...m$ into k clusters are as follows.

1. Initialize cluster number k and cluster center C_j.
2. The data point y_i is assigned to the group that has the closest cluster center.
3. Compute new cluster centers after assigning all the data points to any of the clusters.
4. Steps 2 and 3 are repeated until cluster membership stabilizes.

The goal of k-means algorithm is to minimize an objective function given by,

$$J=\sum_{j=1}^{k}\sum_{i=1}^{m}\left\|y_i-C_j\right\|^2 \quad (1)$$

where $\left\|y_i-C_j\right\|$ is the Eucledian distance between a data point y_i and centroid C_j.

K-means algorithm is also known as hard classification algorithm because it forces every pixel to belong to one and only class in each iteration unlike in soft classification methods [15, 16]. Therefore k-means algorithm is also referred to as a simpler non-probabilistic alternative to Gaussian mixture.

K-means algorithm is applied on pixel values using $k=2$ as the image predominantly consists of two regions as shown in Fig. 2 (a). In our work, we use k-means algorithm in two different samples of the image; only cross-diagonal pixels and the pixels outside the cross-diagonals. The image representation of the proposed approach is shown in Fig. 2 (b). The red lines represents the cross-diagonal pixels and are selected in such a way that it passes through the center of the image. The cross-diagonal pixels help to focus the object of interest as shown in Fig. 2 (b) and makes it more evident. But, the cross-diagonal pixels does not include entire SN, and hence cannot segment them accurately. Therefore, the pixels outside the cross-diagonals are also considered for accurate segmentation. *K*-means is performed for both the samples of the image. The algorithm results in two final centroids represented by C_1 and C_2. The threshold [17-19] T' is calculated as,

$$T'=\frac{C_1+C_2}{2} \quad (2)$$

where $T'=T_d$ represents cross-diagonal pixels and $T'=T_r$ represents pixels outside the cross-diagonals.

The final threshold value T is calculated as,

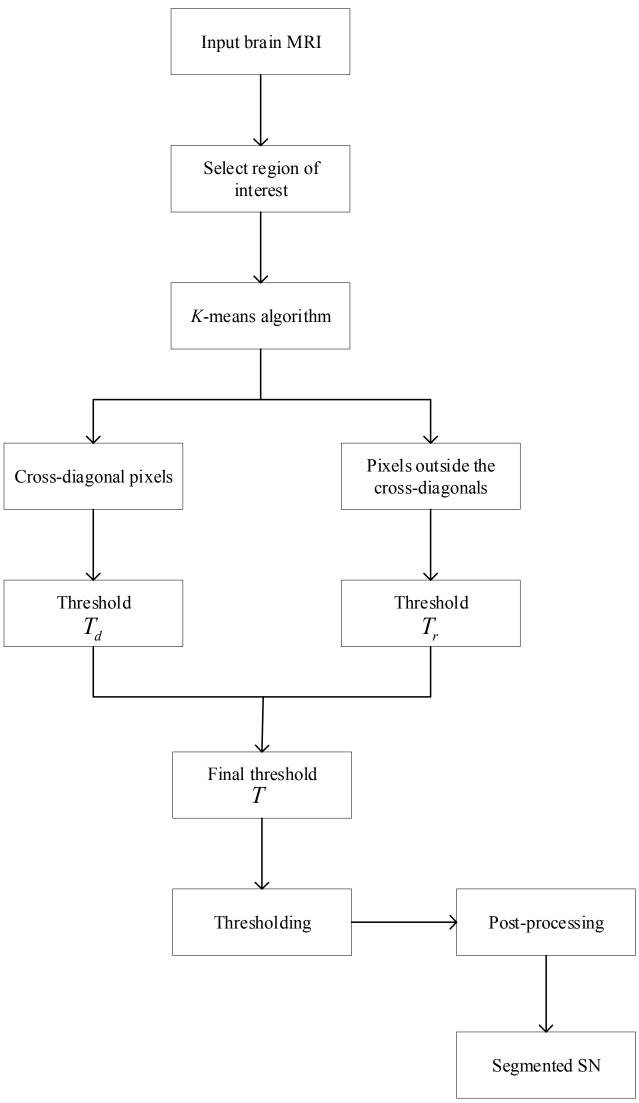

Fig. 1. Flowchart of the proposed method.

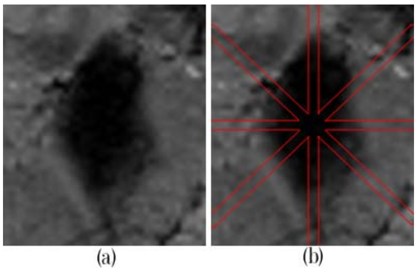

Fig. 2. Image representation for (a) all pixels (b) only cross-diagonal pixels.

$$T = \alpha T_r + (1-\alpha) T_d \tag{3}$$

where α is a constant which balances the two thresholds.

B. Thresholding

Thresholding is a simple, fast and computationally efficient method for image segmentation because it differentiates the gray level of pixels belonging to the object from the gray level of the pixels belonging to the background. Thresholding can be single or multilevel thresholding. In our work, we use single threshold to separate the image into different classes.

SN varies in shape and size and if we sample the image shown in Fig. 3 (a), (all image pixels) we obtain histogram as shown in Fig. 3 (b). The distribution is unimodal and hence histogram thresholding is clearly not possible. On the other hand, a threshold value computed with the help of *k*-means algorithm segments SN as shown in Fig. 3 (c), with the boundary containing some of the irrelevant background pixels. Therefore, we estimate threshold using (3) to categorize the image regions into their respective classes for the effective segmentation. The result of thresholding operation is always a binary image as shown in the Fig. 4 (b).

C. Post-processing

The binary image obtained after the thresholding stage contains many disjoint pixels creating confusion with the object of interest as shown in Fig. 4 (b). Therefore, the goal of the post-processing stage is to remove all the disjoint objects and select the single largest connected region that is likely to be SN which we are trying to segment. The single connected region consists of holes which needs to be filled using morphological reconstruction. Moreover, the single co

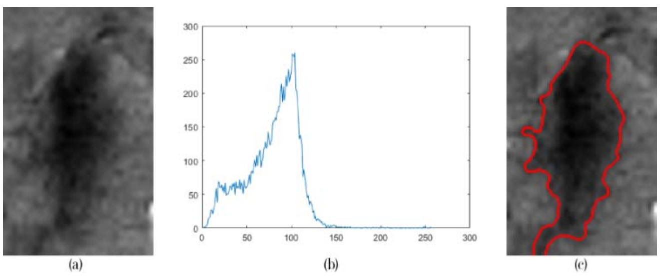

Fig. 3. (a) Input image (b) Histogram of all image pixels. (c) Over-segmented image. *K*-means threshold for all image pixels = 69.

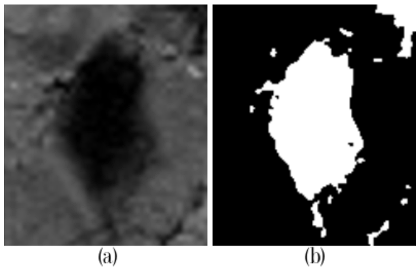

Fig. 4. (a) Input image (b) Binary image. Threshold estimated using the proposed method, T = 0.8 · 44 + (1 − 0.8) · 38 = 42.8 (α = 0.8).

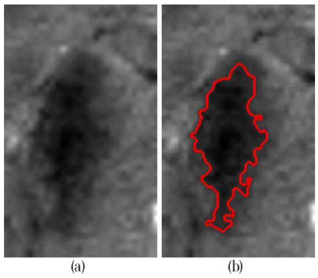

Fig. 5. (a) Input image (b) Segmentation result without Gaussian filtering

-nnected region is not smooth, hence it is smoothened by a Gaussian filter. Fig. 5 (b) shows the result of the segmentation without Gaussian filtering which gives jagged output. Therefore, we use two-dimensional Gaussian low pass filter of size 9×9 to remove the details from the connected region. Finally, we detect the border of the connected region and overlay the input image with the detected border to obtain the desired segmentation result.

Comparison of different methods

We compare the proposed methodology with threshold estimated from all the pixels in the image. Threshold value is computed by *k*-means algorithm using $k=2$. The darker cluster corresponds to the SN, therefore, we also performed comparative analysis using the threshold value of the darker cluster for fair comparison. Moreover, level set method [20] is also used for the comparison, since it is frequently used method for segmenting smaller structures in medical image domain.

III. Results and Discussion

MRI data used in this research is freely available and described in detail by Forstmann et al. [21]. 53 healthy individuals comprising of 30 young, 14 middle-aged and 9 elderly participants were included in the study. The data were generated using a 7 T Siemens Magnetom MRI scanner with a 24-channel head array Nova coil (NOVA Medical Inc., Wilmington MA). The T2*- weighted multi-echo 3D FLASH used the following parameters: repetition time (TR) = 41 ms, bandwidth = 160 Hz/Px, flip angle $=14^{\circ}$, three echo

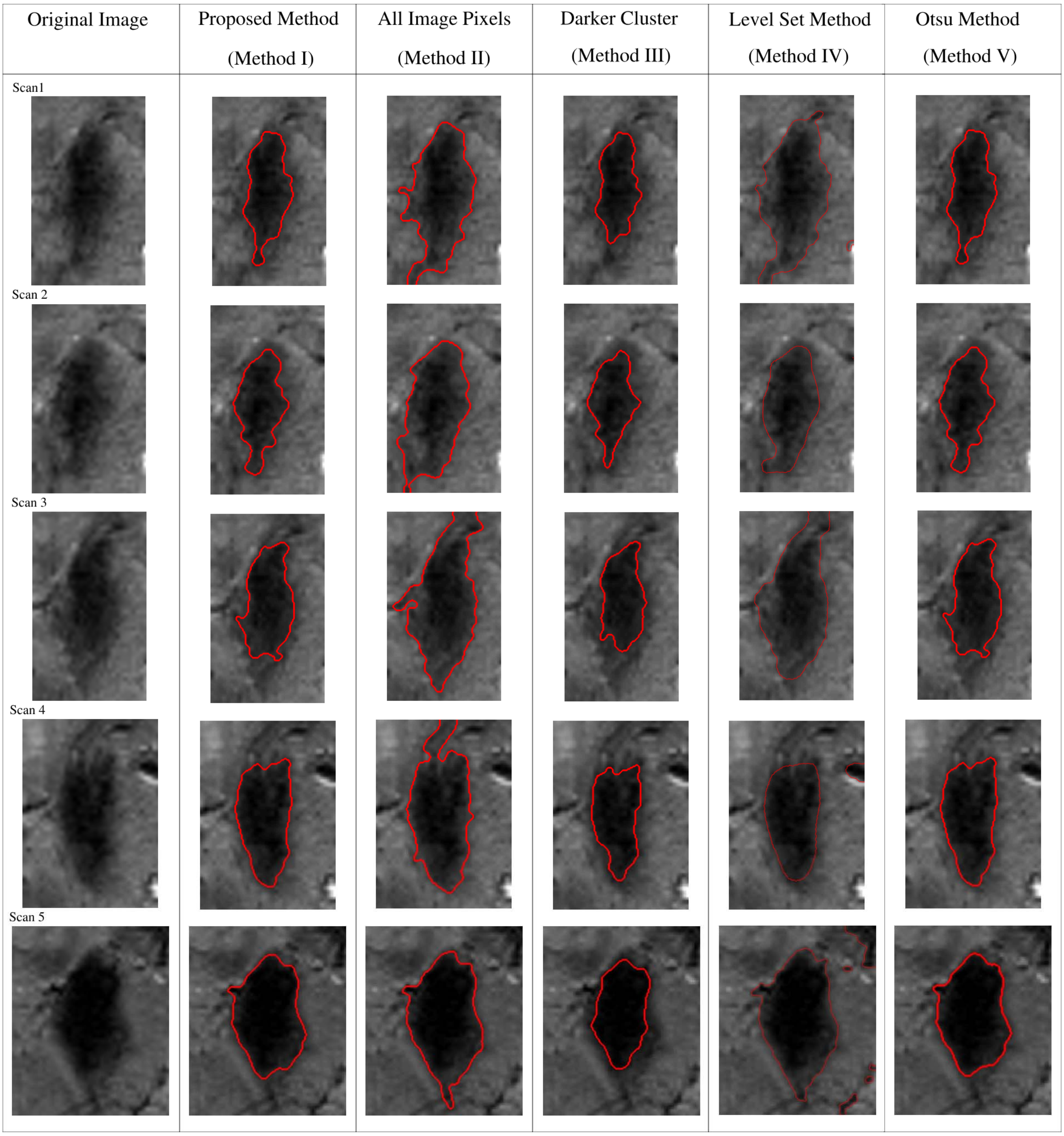

Fig. 6. Comparison of segmentation results of our proposed method with different methods.

times (TE): 11.22/20.39/29.57 ms, voxel size = $(0.5\text{ mm})^3$ and number of slices = 128 tilted at -23 degrees.

The method proposed in this work estimates the threshold value for accurate segmentation of SN using different samples of the image. The threshold estimation also depends on the parameter α . In our experiment, we obtained the best results using $\alpha = 0.80$.

The proposed weighted thresholding method is applied to the data obtained from different age groups including young, middle-aged and elderly participants. The segmentation resul-t of our proposed method along with the comparison to threshold estimated using all image pixels (method II), darker cluster (method III) and level set method (method IV) [20] is shown in Fig. 6. The result of 5 sample scans is shown in the Fig. 6 to illustrate the effectiveness of the proposed algorithm. The area enclosed within the red contours is the final segmentation result generated by each of these methods.

Subjective evaluation is done by an experienced radiologists for the analysis of each of these methods. The subjective evaluation score is shown in Table I. The radiologist gave the highest subjective score to the results ge

TABLE I. SUBJECTIVE EVALUATION SCORES

SCAN NUMBER	RATINGS (1-5)			
	Method I	*Method II*	*Method III*	*Method IV*
Scan 1	3	1	2	1
Scan 2	3	2	2	3
Scan 3	3	1	2	2
Scan 4	4	1	2	3
Scan 5	4	2	1	2

Note: 1: Lowest

5: Highest

-nerated by our proposed algorithm. The proposed method enclosed better SN area than the rest of the methods according to the radiologist perspective. The segmentation results of the proposed method was closer to manual segmentation than the other methods. Method II, Method III and method IV constantly overestimated and under segmented object of interest as well as included those areas which cannot be referred as SN.

The study proposed a novel segmentation algorithm of using weighted sum of threshold estimated along the cross-diagonal pixels and the pixels outside the cross-diagonals for calculating the final threshold value that works well for the segmentation of SN which is an important measure for the analysis of PD. To show the superiority of the proposed method, comparison to the result of the threshold estimated using all image pixels is also shown in Fig. 6 which clearly could not segment SN. In fact, it covered many other irrelevant areas. We also performed comparative analysis using the threshold value of the darker cluster but it under segmented the object of interest. Level set method is also used for the comparison with our proposed method but it could not segment SN accurately. Additionally, level set method requires fine tuning of various parameters. Hence, the proposed method has a superior hold over other methods and it validates our proposed methodology.

Otsu thresholding [22] was also used for the estimation of threshold in our proposed work because it is one of the most successful method for image segmentation based on minimizing within-class variance. Otsu thresholding estimated the threshold value similar to *k*-means algorithm. Therefore, the segmentation result of Otsu method and our proposed method is similar and is also shown in Fig. 6. However, it should be noted that Otsu method is an exhaustive search algorithm that finds the global optimal threshold while *k*-means is a local optimal method. Moreover, *k*-means runs faster [18] than the Otsu method. Similarly, *k*-means thresholding is a general method as it does not require a histogram before calculation.

In the proposed methodology, the width of the cross-diagonals also affects the result. We dilate cross-diagonal pixels with an appropriate structuring element. In our work, we obtain the best result with disk structuring element of radius r, where $2 \leq r \leq 4$. The structuring element of radius greater than this range results in an inaccurate segmentation of SN. Additionally, we also assume that the object of interest lies approximately in the center of the image. Hence, the ROI is selected in such a way that the object of interest lies almost in the center of the image.

However, like in any other medical imaging applications, the difficulty of selecting the ground truth exists. Hence, selecting an appropriate ground truth image and performing the quantitative evaluation will be the future direction of research in addition to developing a more robust and improved algorithm for the SN segmentation. Moreover, performing volumetric analysis and studying morphometric variability of SN will be the future direction of research which can provide insight to PD characteristics and progression.

IV. Conclusion

We proposed a novel algorithm for SN segmentation using thresholding operation based on *k*-means algorithm. The proposed method of using weighted sum of threshold computed along the cross-diagonal pixels and the pixels outside the cross-diagonals for calculating the final threshold value works well for segmentation of SN as is evident by the experimental results. The proposed algorithm produces results closer to manual segmentation than the general thresholding methods and level set method. The subjective evaluation performed by an experienced radiologist supports our claim and validates the proposed methodology.

As seen in Fig 3 (b), the histograms of the ROI samples are skewed towards the darker side of the intensity range and offers the possibility of contrast stretching. However, the end result of the segmentation of SN was not significantly different from those obtained using the proposed method.

References

[1] J. M. Fearnley, and A. J. Lees, “Ageing and Parkinson's disease: substantia nigra regional selectivity,” *Brain,* vol. 114 (Pt 5), pp. 2283-301, Oct, 1991.

[2] B. Hallgren, and P. Sourander, “The effect of age on the non-haemin iron in the human brain,” *J Neurochem,* vol. 3, no. 1, pp. 41-51, Oct, 1958.

[3] E. Sofic, W. Paulus, K. Jellinger, P. Riederer, and M. B. Youdim, “Selective increase of iron in substantia nigra zona compacta of parkinsonian brains,” *J Neurochem,* vol. 56, no. 3, pp. 978-82, Mar, 1991.

[4] R. A. Menke, S. Jbabdi, K. L. Miller, P. M. Matthews, and M. Zarei, “Connectivity-based segmentation of the substantia nigra in human and its implications in Parkinson's disease,” *Neuroimage,* vol. 52, no. 4, pp. 1175-80, Oct 1, 2010.

[5] Y. Xiao, L. Bailey, M. M. Chakravarty, S. Beriault, A. F. Sadikot, G. B. Pike, and D. L. Collins, "Atlas-Based Segmentation of the Subthalamic Nucleus, Red Nucleus, and Substantia Nigra for Deep Brain Stimulation by Incorporating Multiple MRI Contrasts," *Information Processing in Computer-Assisted Interventions*. pp. 135-145.

[6] C. Haegelen, P. Coupe, V. Fonov, N. Guizard, P. Jannin, X. Morandi, and D. L. Collins, “Automated segmentation of basal ganglia and deep brain structures in MRI of Parkinson's disease,” *Int J Comput Assist Radiol Surg,* vol. 8, no. 1, pp. 99-110, Jan, 2013.

[7] Y. Xiao, P. Jannin, T. D'Albis, N. Guizard, C. Haegelen, F. Lalys, M. Verin, and D. L. Collins, “Investigation of morphometric variability of subthalamic nucleus, red nucleus, and substantia nigra in advanced Parkinson's disease patients using automatic segmentation and PCA-based analysis,” *Hum Brain Mapp,* vol. 35, no. 9, pp. 4330-44, Sep, 2014.

[8] J. Kim, C. Lenglet, Y. Duchin, G. Sapiro, and N. Harel, "Semiautomatic segmentation of brain subcortical structures from high-field MRI," *IEEE J Biomed Health Inform,* vol. 18, no. 5, pp. 1678-95, Sep, 2014.

[9] E. Visser, M. C. Keuken, B. U. Forstmann, and M. Jenkinson, "Automated segmentation of the substantia nigra, subthalamic nucleus and red nucleus in 7 T data at young and old age," *Neuroimage,* vol. 139, pp. 324-336, Oct 1, 2016.

[10] T. Guo, Y. Song, J. Li, M. Fan, X. Yan, A. He, D. Huang, C. Shen, G. Zhang, and G. Yang, "Seed point discontinuity-based segmentation method for the substantia nigra and the red nucleus in quantitative susceptibility maps," *J Magn Reson Imaging*, Mar 31, 2018.

[11] A. K. Jain, "Data clustering: 50 years beyond K-means," *Pattern Recognition Letters,* vol. 31, no. 8, pp. 651-666, 2010/06/01/, 2010.

[12] M. Laszlo, and S. Mukherjee, "A genetic algorithm using hyper-quadtrees for low-dimensional k-means clustering," *IEEE Transactions on Pattern Analysis and Machine Intelligence,* vol. 28, no. 4, pp. 533-543, 2006.

[13] J. Liu, and L. Guo, "A New Brain MRI Image Segmentation Strategy Based on K-means Clustering and SVM." pp. 270-273.

[14] H. P. Ng, S. H. Ong, K. W. C. Foong, P. S. Goh, and W. L. Nowinski, "Medical image segmentation using K-MEANS clustering and improved watershed algorithm," *7th Ieee Southwest Symposium on Image Analysis and Interpretation*, pp. 61-+, 2006.

[15] M. A. M. a. K. Kalti, "Image segmentation by adaptive distance based on EM algorithm," *CoRR*, 2012.

[16] S. Shan, W. Sandham, M. Granat, and A. Sterr, "MRI fuzzy segmentation of brain tissue using neighborhood attraction with neural-network optimization," *IEEE Transactions on Information Technology in Biomedicine,* vol. 9, no. 3, pp. 459-467, 2005.

[17] Z.-K. Huang, and K.-W. Chau, "A new image thresholding method based on Gaussian mixture model," *Applied Mathematics and Computation,* vol. 205, no. 2, pp. 899-907, 2008/11/15/, 2008.

[18] D. J. Liu, and J. A. Yu, "Otsu method and K-means," *His 2009: 2009 Ninth International Conference on Hybrid Intelligent Systems, Vol 1, Proceedings*, pp. 344-349, 2009.

[19] M. Zortea, E. Flores, and J. Scharcanski, "A simple weighted thresholding method for the segmentation of pigmented skin lesions in macroscopic images," *Pattern Recognition,* vol. 64, pp. 92-104, 2017/04/01/, 2017.

[20] C. Li, R. Huang, Z. Ding, J. C. Gatenby, D. N. Metaxas, and J. C. Gore, "A level set method for image segmentation in the presence of intensity inhomogeneities with application to MRI," *IEEE Trans Image Process,* vol. 20, no. 7, pp. 2007-16, Jul, 2011.

[21] B. U. Forstmann, M. C. Keuken, A. Schafer, P.-L. Bazin, A. Alkemade, and R. Turner, "Multi-modal ultra-high resolution structural 7-Tesla MRI data repository," *Scientific Data,* vol. 1, pp. 140050, 12/09/online, 2014.

[22] N. Otsu, "A Threshold Selection Method from Gray-Level Histograms," *IEEE Transactions on Systems, Man, and Cybernetics,* vol. 9, no. 1, pp. 62-66, 1979.